RESEARCH ARTICLE

www.mundonano.unam.mx | **Mundo Nano**
https://doi.org/10.22201/ceiich.24485691e.2024.33.69810 | **17(33), 1e-13e, July–December 2024**

H_2S removal at downhole conditions using iron oxide nanoparticles◊

Remoción de H_2S en condiciones de fondo de pozo empleando nanopartículas de óxido de hierro

Luis A. Meléndez Santana,*,♦ Julia T. Guerra Hernández,* Claudio G. Olivera-Fuentes*

ABSTRACT: The objective of the present work is the study of H_2S removal from heavy oil, using iron oxide nanoparticles in a controlled environment that simulates the pressure and temperature conditions of a reservoir and the aqua-thermolysis process during enhanced oil recovery with steam injection. Since molecular diffusion of H_2S plays an important role during the removal process, its measurement through experimental tests was also a major goal. The research divides into three stages: 1) preparation of nanoparticles; 2) diffusion tests, and, 3) H_2S removal tests. The procedure for nanoparticle preparation from a microemulsion and a metal precursor salt was successful in yielding nanoparticle sizes less than 100 nm. The diffusion coefficient of H_2S in heavy oil, measured in a stainless steel PVT cell, varied between 8.3×10^{-9} and 8.9×10^{-9} m^2s^{-1} over the range of test temperatures. Finally, over 65% of the H_2S was removed when 500 ppm of nanoparticles were used.
KEYWORDS: iron oxide nanoparticles, preparation, H_2S, diffusion, *in situ* removal, enhanced oil recovery (EOR).

RESUMEN: El objetivo del presente trabajo es el estudio de la remoción de H_2S de crudos pesados empleando nanopartículas de óxido de hierro en un ambiente controlado que simula las condiciones de presión y temperatura de un yacimiento y el proceso de acuatermólisis durante la recuperación mejorada de petróleo con inyección de vapor. Dado que la difusión molecular del H_2S tiene un rol importante en el proceso de remoción, su medición experimental fue también un objetivo principal. La investigación se desarrolló en tres etapas: 1) preparación de las nanopartículas; 2) ensayos de difusión, y, 3) ensayos de remoción de H_2S. El protocolo de síntesis de las nanopartículas a partir de una microemulsión y una sal metálica precursora generó exitosamente nanopartículas de tamaños inferiores a 100 nm. El coeficiente de difusión del H_2S en el crudo pesado, medido en una celda PVT de acero inoxidable, varió entre 8.3×10^{-9} y 8.9×10^{-9} m^2s^{-1} en el rango de temperaturas de las pruebas. Finalmente, más del 65% del H_2S fue removido al usar 500 ppm de nanopartículas.
PALABRAS CLAVE: nanopartículas de óxido de hierro, síntesis, H_2S, difusión, remoción *in situ*, recuperación mejorada de petróleo (EOR).

Received: August 2, 2022. Accepted: November 17, 2023. Published: January 22, 2024.

◊ The authors are grateful to the Venezuelan Institute of Petroleum Technology (INTEVEP) for provision of the research facilities where the experimental stages of this work carried out. The leading author, Luis A. Meléndez Santana, acknowledges the constant support and encouragement of PhD Susana Martínez at INTEVEP.
* Universidad Simón Bolívar, Departamento de Termodinámica y Fenómenos de Transferencia, Caracas, Venezuela.
♦ Correspondence author: luissantana123@gmail.com

Introduction

Steam injection as an enhanced oil recovery (EOR) method for heavy and extra heavy oil involves several challenges. One of them is handling the H_2S produced by the rupture of C-S bonds at high temperatures and pressures (greater than 200 ºC and 1000 psig) prevailing at the bottom of the well. This process, known as aqua-thermolysis (Husein *et al*., 2010), generates H_2S and other pollutants such as CO_2, which poses risks to the health of workers, the environment, the facilities, and the surface equipment that transports the crude from the well to the separation and treatment units. The H_2S concentration can exceed 3,000 ppm, depending on the reservoir and the characteristics of the crude (Zhu *et al*., 2010). In the specific case of developments in the Orinoco Oil Belt, Venezuela, this has prompted the development of previous H_2S production and management studies (Mi *et al*., 2017).

The removal of H_2S has been extensively studied and there are mature technologies for treatment and conversion to elemental sulphur downstream of oil production. Reversible processes based on liquid sorbents use mainly mono-, di- and tri-ethanolamines (MEA, DEA, TEA), while non-reversible technologies based on solid sorbents employ metal oxides. The first developments in H_2S scavenging with metallic oxides were based on copper compounds added to water-based drilling muds, which caused the precipitation of H_2S as insoluble copper sulphide; however, their use is seriously limited by corrosion problems that they cause in ferrous materials. As an alternative, the use of zinc oxide and zinc carbonate also showed good performance over a wide pH range, but high zinc ion concentrations are required to achieve high removal efficiency, and this affects the rheological properties of the drilling mud, so its use is limited. Iron compounds such as magnetite and ferrous gluconate could offer better performance at low pH values (Amosa *et al*., 2010).

Using iron oxide nanoparticles for *in situ* H_2S removal offers an alternative to mitigate H_2S production. The reaction process does not generate by-products, and, because of the large specific surface area of the nanoparticles, they can be used at low concentrations and there is no need to recover them (Martínez and Bastidas, 2017). Although zinc oxide in drilling fluids reacts faster than iron oxide, the latter yields higher amount of H_2S removed per unit mass, especially at lower pH values (Evers and Olson, 1983). However, since the rate of diffusion of H_2S in heavy oil is very low, a poor distribution of the iron oxide in the crude oil would decrease the probability of collisions between H_2S molecules and nanoparticles during oil production. For this reason, it is important to achieve good dispersion of the nanoparticles, to avoid possible limitations on the process efficiency because of the diffusion velocity of H_2S in the oil (Nassar *et al*., 2010).

The present work involves assess the removal of H_2S in heavy crude oils by using iron oxide nanoparticles injected downhole. The H_2S reacts with

nanoparticles in such a way that they form stable compounds, which safely, during the entire process of transporting crude oil to the processing plants can handled.

Preparation of nanoparticles

Nanoparticles were synthesised using a procedure described by Capek (2004) and Martínez & Bastidas (2017). A microemulsion was prepared in a batch reactor using a mixture of aromatic solvents, a metal precursor salt was added to it, and the reaction temperature was adjusted between 200 and 280 °C for 24 h. The nanoparticles obtained by this process had sizes less than 100 nm and were characterized by high-resolution transmission electron microscopy (HRTEM). Figure 1 shows an HRTEM image of the nanoparticle solution. Variable sizes below 20 nm were observed.

An X-ray diffraction analysis (XRD) was carried out to determine the crystallographic structure of the nanoparticles. The diffraction pattern obtained was compared with the database associated with the Match application in its free version (International Centre for Diffraction Data, 2023), which uses the ICDD database for XRD of powders, so that it was possible to corroborate the coincidence of the lines of highest intensity with the pattern reported with #96-900-0927 corresponding to a cubic Magnetite (Fe_3O_4), the coincidence of lines was 100%, thus indicating that there is a pure phase of the solid (figure 2). The signal's low intensity and bandwidth indicate the presence of highly dispersed nanometric particles in the reaction medium. These results are consistent with the shown by HRTEM analysis where particle sizes between 20-50 nm were achieved (figure 1).

FIGURE 1. Transmission electron microscopy (MET AR) high resolution of nanoparticles.

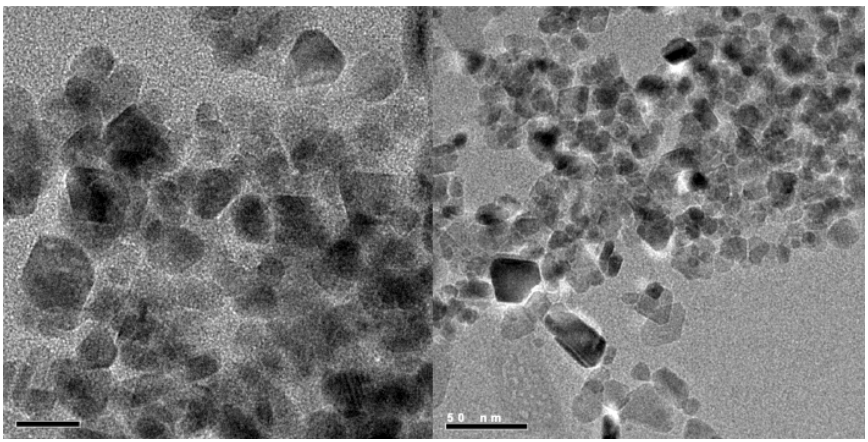

Source: Author's elaboration.

FIGURE 2. Diffractogram DRX of nanoparticles sample.

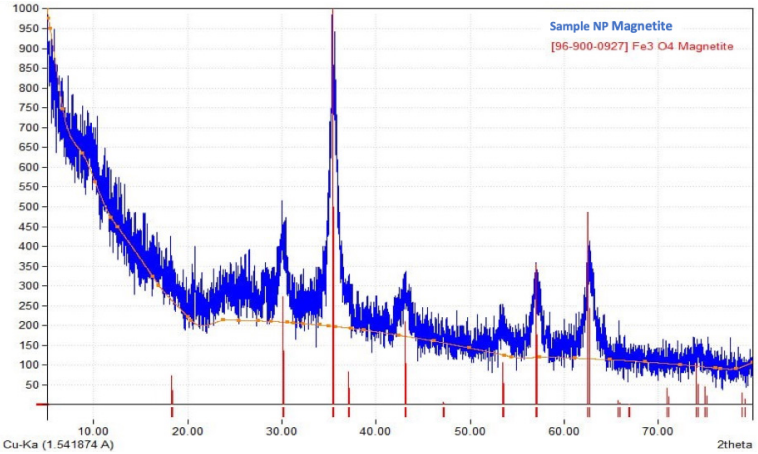

Source: https://www.crystalimpact.com/news/20231010a.htm.

Diffusion tests

A stainless steel PVT cell was manufactured with a height of 10 cm and an internal diameter of 4.5 cm. Pure H_2S and 8.5°API heavy oil were used. The cell was placed in vertical position and tests were carried out at four different temperatures (40, 50, 60, and 70 °C). The temperature remained constant throughout the test.

The diffusion coefficient of the dissolved H_2S was inferred by an indirect method proposed by Riazi (1996). This involved monitoring the pressure decrease of the gas, which depends on the rate of mass transfer across the gas-liquid interface. Assuming the validity of the penetration model for unsteady-state one-dimensional diffusion in a liquid region of finite constant depth, Fick's second law is written as:

$$\frac{\partial c_A}{\partial t} = D_{Am} \frac{\partial^2 c_A}{\partial z^2} \tag{1}$$

With initial and boundary conditions:

$$\begin{aligned} c_A &= 0 \quad @ \quad t = 0, all\ z \\ c_A &= c_{A,sat} \quad @ \quad t > 0, z = z_0 \\ \frac{\partial c_A}{\partial z} &= 0 \quad @ \quad t > 0, z = 0 \end{aligned} \tag{2}$$

Where $0 \leq z \leq z_0$ is the liquid height, c_A is the molar concentration of the dissolved gas, $c_{A,sat}$ is its composition at saturation (solubility), and D_{Am} is its effective diffusivity in the liquid at the cell temperature T and pressure P.

In principle, the height z_0 of the liquid phase could increase as the gas dissolves, because its total mass goes up and its density goes down (swelling effect). However, the solubility of H_2S in heavy crude oil is low, therefore this effect was considered negligible in the present case. The solution of Eq (1) subject to Eq (2) is well known, e.g. Crank (1975). Of particular interest is the composition gradient at the interface, given by

$$\left.\frac{\partial c_A}{\partial z}\right|_{z=z_0} = \frac{2c_{A,sat}}{z_0}\sum_{n=0}^{\infty} exp\left[-\left(\frac{(2n+1)\pi}{2z_0}\right)^2 \mathcal{D}_{Am}t\right] \tag{3}$$

The pressure change in the gas phase follows from a molar balance (Zhang *et al*., 2000) as

$$\frac{d}{dt}\left(\frac{PhA}{ZRT}\right) = -\mathcal{D}_{Am}A\left.\frac{\partial c_A}{\partial z}\right|_{z=z_0} \quad \rightarrow \quad dP = -\frac{ZRT}{h}\mathcal{D}_{Am}\left.\frac{\partial c_A}{\partial z}\right|_{z=z_0} dt \tag{4}$$

where h is the height of the gas space above the liquid, Z is the gas compressibility factor, and A is the cell cross-sectional area, all of which are taken to be constant. At sufficiently long times, the series in Eq (3) can be approximated by its leading term, and integration of Eq (4) from such large values of t up to infinity yields

$$ln[P(t) - P_{sat}] = ln\frac{8ZRTz_0c_{A,sat}}{\pi^2 h} - \frac{\pi^2\mathcal{D}_{Am}}{4z_0^2}t \tag{5}$$

Which has the form: $f(t) = A + Bt$.

Given the liquid height z_0 in the cell, the diffusion coefficient can thus be determined from the end slope of the line obtained by plotting the experimental pressure data against time according to Eq (5). No detailed knowledge of the parameters that make up the intercept A is necessary. The saturation pressure P_{sat} must be known, however, but this is the limiting pressure observed at equilibrium after appropriately long run times (4 days in the present work.) The slope of the curve is sensitive to small changes in the saturation pressure (Zhang *et al*., 2000), so measurements should be replicated whenever possible.

Shown in figure 3 is the pressure behaviour *versus* time. Eight tests were carried out at 40, 50, 60, and 70 °C. Initially, when the gas and the oil come into contact, the pressure drops rapidly, about a quarter or a third of the overall change. This is known as the "incubation period", and was observed during the first 30 to 60 min, time necessary for H_2S to dissolve at the gas/liquid interface, establish the boundary condition, and diffuse down to create the composition profile over the entire liquid depth. The slope of the curve described in Eq (5) should remain linear until H_2S reaches the opposite end of the PVT cell. The truncated form of Eq (3) cannot described the high curvature in these early stages, and is as well visible in the linearized coordinates of Eq (5), as shown in figure 4. Points in the incubation period were therefore omitted from the statistical analysis of the data. Pomeroy *et*

al. (1933) showed that this assumption is reasonable and introduces negligible uncertainties in the interpretation of the data.

The data in the incubation period could possibly be analysed by an alternative "penetration" model, that treats the liquid phase as an infinitely deep pool, but this was unnecessary because the diffusivity of H_2S in the crude oil could be obtained directly from the linear regression, as described in the literature cited and confirmed in our work. Least squares regression using the MATLAB® tool yielded linear fits with regression coefficients better than 0.980. The initial and final pressures, and the computed diffusion coefficients are listed in table 1. The pressure change was 426 kPa on average. Mean diffusivities vary between 8.3×10^{-9} and 8.9×10^{-9} m^2s^{-1} from 40 to 70 °C, with a low outlier from a single run at 50 °C. These values are consistent with those reported for the diffusivity of other gases in heavy oil fractions, e.g. CO_2 (Upreti and Mehrotra, 2000) and CO, CH_4, C_2H_6, N_2 (Upreti and Mehrotra, 2002).

FIGURE 3. Gas pressure as a function of time. Diffusion tests at 40, 50, 60 and 70 °C.

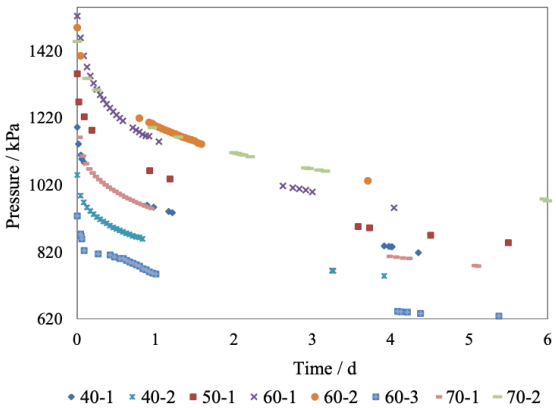

Source: Author's elaboration.

FIGURE 4. Linear fit of pressure data as a function of time (for 40, 50, 60 and 70 °C).

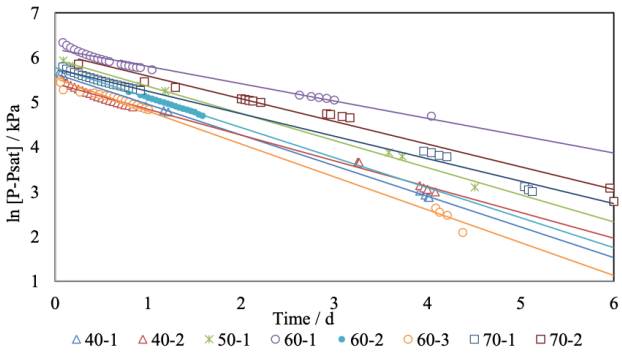

Source: Author's elaboration.

TABLE 1. H_2S–oil diffusion coefficient as a function of temperature.

Test run	T / °C	$P(t = 0)$ / *kPa*	P_{sat} / *Pka*	$10^9 D_{Am}$ / $m^2 s^{-1}$	$10^9 D_{Am,ave}$ / $m^2 s^{-1}$
40-1 40-2	40	1192 1048	818 745	7.90 8.71	8.31
50-1	50	1351	848	7.35	7.35
60-1 60-2 60-3	60	1524 1489 927.3	952 1032 628.5	8.17 8.89 8.51	8.52
70-1 70-2	70	1162 1448	778 972	8.78 8.94	8.86

Source: Author's elaboration.

H_2S removal tests

Three stages make up the H_2S mitigation test: 1) conditions for maximum H_2S production; 2) optimal concentration of nanoparticles, and, 3) quantification of H_2S removal.

Maximum H_2S production

The main source of H_2S production in EOR of oil fields is thermochemical sulphate reduction (TSR) at the high temperatures reached. The amount of H_2S generated depends on the oil contents of sulphur compounds, injection temperature, and rock composition and physicochemical properties (Mi *et al*., 2017). Tests were carried out in four autoclaves of 600 mL internal volume, each charged with 90 g of heavy oil, 10 g of water and 150 psig (1136 kPa) of 99.9 vol% methane. They heated up to 250, 280, 300, and 320 °C, respectively, and kept isothermal during a reaction time of 15 h, after which gas samples were drawn and analysed for H_2S concentration. A considerable increase in H_2S evolution was detected, from less than 100 ppm at 280 °C to 1200 ppm at 300 °C, and slightly above 10,000 ppm at 320 °C (figure 5). These values are consistent with previous reports by Mi *et al*. (2017) for the same crude, and may serve as a guideline for setting the steam injection temperature in an EOR process if excessive downhole H_2S production avoided.

Optimal nanoparticle concentration

In order to determine the optimal concentration of nanoparticles, four autoclaves of 600 mL internal volume were each charged with 90 g heavy oil, 10 g water, 150 psig (1136 kPa) of 99.9 vol% methane, and zero (control blank), 250, 500 and 1000 ppm of nanoparticles, respectively. All tests carried out in duplicate, and, once completed, gas samples for total sulphur analysis using the ASTM D2622 standard were drawn. The gas chromatographic analysis followed the UOP 539-12 standard, and H_2S concentration was measured using sulphide colorimetric detector tubes. The reacted nanoparticles were extrac-

FIGURE 5. H_2S generated at different temperatures (reaction time 15 hours).

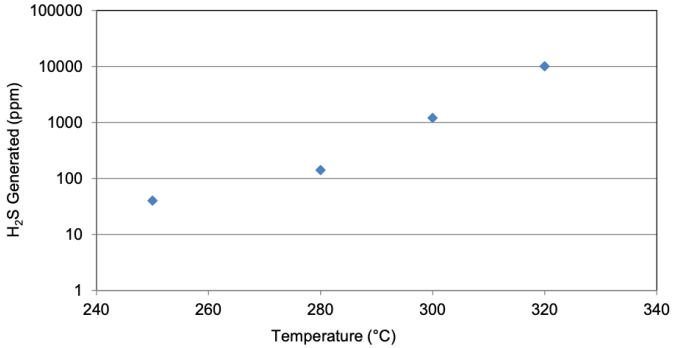

Source: Author's elaboration.

ted by washing with toluene and subjected to centrifugation to be analysed by electron microscopy.

Figure 6 shows the production of H_2S for the four samples and the percentages of gas removed, which were 77.2, 92.6 and 88.2 % for the respective samples containing 250, 500 and 1000 ppm of iron oxide nanoparticles. Although this last result is not conclusive, due to the few tests carried out, an agglomeration of the nanoparticles may have occurred at the higher concentration, thereby decreasing the contact area and, consequently, the removal of H_2S. On the basis of these results, it was decided to use only 500 ppm of nanoparticles in the subsequent removal tests, to be performed at 300 °C with reaction times up to 160 h.

FIGURE 6. H_2S production and percent removal for different concentrations of nanoparticles.

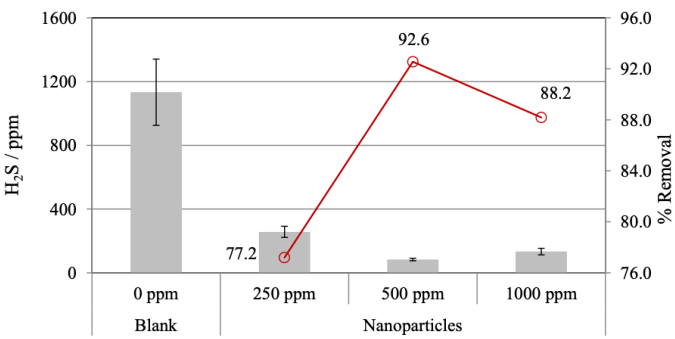

Source: Author's elaboration.

H_2S removal

Figure 7 exhibits the H_2S generated with nanoparticles ("additive") and without them. The H_2S generated without additive increased from 40 to 1000 ppm for reaction times from 15 to 160 h. In the same way, the removal rate with addi-

FIGURE 7. Generation and percent removal of H_2S as a function of reaction time.

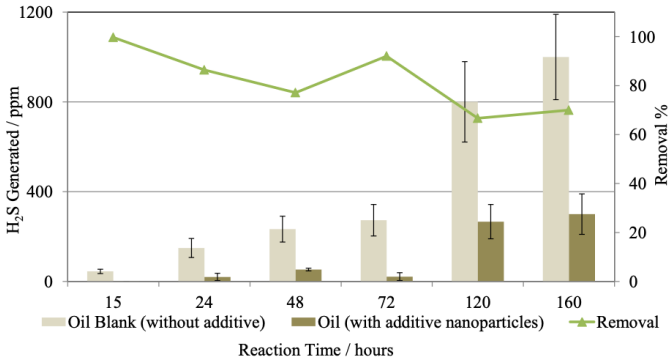

Source: Author's elaboration.

tive, the decrease from 99.8 % to about 70 %, with some dispersion, but in any case, exceeding 65 %.

When chromatographic analysis of the reaction gases was made —tests at 15, 48 and 72 h—, the iron oxide additive works not only as an agent for removing H_2S molecules, but also promotes the production of light compounds. Composites such as propane, propylene, butane, pentane and hydrogen, which indicates that there was cracking of the oil samples and, possibly, an improvement in their viscosity (table 2).

Samples taken from the reacted oil and analysed for total sulphur contents, confirmed a reduction in sulphur percentage by comparison with the unreacted crude. As shown in figure 8, this decrease was greater for the blank samples than for those with additive, but this is just because the H_2S generated during the aqua-thermolysis process diffuses into the oil, where it reacts with the iron oxide present to form stable iron sulphide species that are subsequently quantified in the total sulphur analysis.

Finally, the nanoparticles sampled and analysed by scanning electron microscopy (SEM), which showed particle sizes between 0.1 and 1 μm. Their elemental composition was determined by microanalysis using energy dispersion X-ray (EDX) spectroscopy. As expected, the unreacted nanoparticles were mostly composed of oxygen and iron, while the amount of sulphur in the reacted solid increased with time from 7.35 to 13.08 %, which confirms that H2S diffuses into the oil and reacts with the iron oxide nanoparticles (table 3).

Conclusions

The use of iron oxide nanoparticles proved to be effective for *in situ* scavenging of H_2S produced by aqua-thermolysis at simulated downhole conditions. At a concentration of 500 ppm, the nanoparticles yielded over 65% reduction of the H_2S generated, with bonus formation of lighter compounds

TABLE 2. Chromatographic composition of reaction gas.

GAS	15 hours		48 hours		72 hours	
	Without nanoparticles	With nanoparticles	Without nanoparticles	With nanoparticles	Without nanoparticles	Without nanoparticless
C6+	0.0	0.024	0.0	0.0004	0.0	0.059
Methane	92.27	93.80	95.21	96.56	94.25	76.27
Ethane	0.0	0.0	0.0	0.0	0.0	7.65
Ethylene	0.0	0.045	0.0	0.00	0.0	0.0
Propane	0.0	0.294	0.0	0.009	0.0	3.71
Propylene	0.0	0.079	0.0	0.0	0.0	0.02
I-Butane	0.0	0.041	0.0	0.0	0.0	0.52
N-Butane	0.0	0.0	0.0	0.005	0.0	0.77
Propadiene	0.0	0.0	0.0	0.0	0.0	0.0
Acetylene	0.0	0.0	0.0	0.0	0.0	0.0
TR2-Butene	0.0	0.012	0.0	0.0	0.0	0.005
1-Butene	0.0	0.022	0.0	0.0	0.0	0.0
I-Butene	0.0	0.046	0.0	0.0	0.0	0.0
CS-2-Butene	0.0	0.008	0.0	0.0	0.0	0.0
I-Pentane	0.0	0.033	0.0	0.0	0.0	0.18
N-Pentane	0.0	0.042	0.0	0.0	0.0	0.15
13-Butadiene	0.0	0.000	0.0	0.0	0.0	0.0
3-ME-1-Butene	0.0	0.000	0.0	0.0	0.0	0.0
TR-2-Pentene	0.0	0.000	0.0	0.0	0.0	0.0
2-ME-2-Butene	0.0	0.000	0.0	0.0	0.0	0.0
1-Pentene	0.0	0.008	0.0	0.0	0.0	0.0
2-ME-1-Butene	0.0	0.009	0.0	0.0	0.0	0.0
CS-Pentene	0.0	0.000	0.0	0.0	0.0	0.0
CO2	0.0	0.018	0.0	0.0	0.0	0.37
Oxygen/ar	2.63	2.053	0.39	2.08	0.34	1.93
Nitrogen	5.09	2.87	3.86	1.26	4.99	4.47
Hydrogen	0.00	0.60	0.54	0.09	0.42	3.91
Total	100.0	100.0	100.0	100.0	100.0	100.0

Source: Author's elaboration.

FIGURE 8. Total sulphur analysis of reacted oil samples.

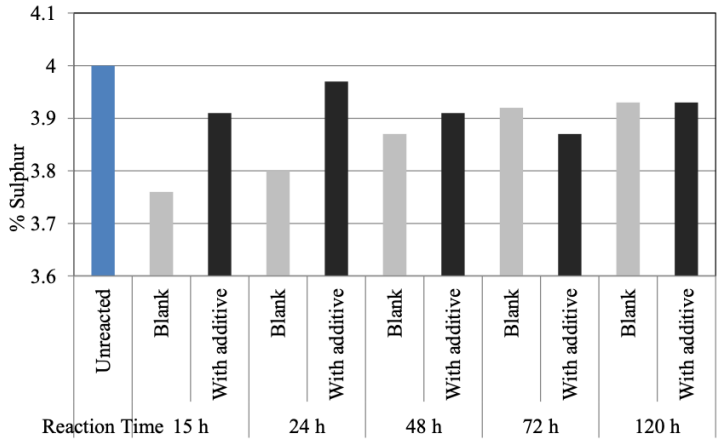

Source: Author's elaboration.

TABLE 3. Microanalysis of nanoparticles by X-ray dispersion spectroscopy of energy (EDX).

Element	Nanoparticles without reaction		Reacted nanoparticles					
			48 hours		72 hours		120 hours	
	weight %	atomic %	weight %	atomic %	weight %	atomic %	weight %	atomic %
O	50.81	78.42	33.3	58.77	43.34	66.65	27.17	11.77
Na	0	0	3.91	4.81	6.76	7.24	9.3	11.84
Si	0	0	0.92	0.93	0	0	0	0
S	0	0	7.35	6.47	7.94	6.09	13.08	11.84
Cl	0	0	4.00	3.18	2.79	1.93	3.03	2.49
K	0	0	0.51	0.37	0.59	0.37	0	0
Ca	0	0	1.63	1.15	0		4.55	3.31
Cr	0	0	1.52	0.82	0.96	0.46	0	0
Fe	46.34	20.49	42.59	21.53	27.46	12.1	24.99	13.03
Ni	0	0	2.55	1.23	5.99	2.51	1.67	0.83
Zn	1.42	0.54	1.71	0.74	2.45	0.92	3.32	1.52
Cu	1.43	0.55	0	0	0	0	12.94	5.76
Mg	0	0	0	0	1.71	1.73	0	0

Source: Author's elaboration.

by cracking long hydrocarbon chains, as evidenced by the presence of alkenes and hydrogen, which may promote a reduction in oil viscosity. Higher concentrations were not used because they appeared to be less effective, possibly due to particle agglomeration, but might be practicable if good dispersion of the nanoparticles in the crude oil can be achieved in industrial practice. This may be desirable since the percent recovery tended to be lower at high rates of H_2S production, which might indicate a limited capacity for reaction yield at the amount of nanoparticles used in this work. Steam injection temperatures in enhanced oil recovery (EOR) processes must not exceed 280 °C to avoid a high production of H_2S.

As part of this study, the diffusion coefficient of H_2S in crude oil was found to range from 8.3 $\times 10^{-9}$ to 8.9 $\times 10^{-9}$ $m^2 s^{-1}$ between 40 and 70 °C. To the best of our knowledge, these are the first reported values for the diffusivity of this gas in a heavy oil. Finally, as irrefutable proof, the analysis of electron microscopy confirms that H_2S diffuses into the oil and reacts with the iron oxide nanoparticles, demonstrating their enormous potential to be used downhole during enhanced oil recovery (EOR).

List of symbols

A	cell cross sectional area, m^2
c_A	dissolved gas concentration, mol/m^3
$c_{A,sat}$	gas solubility, mol/m^3
D_{Am}	diffusion coefficient, m^2/s
h	height of gas space, m
P	pressure, kPa
P_{sat}	saturation pressure, kPa
R	universal gas constant, $(kPa.m^3)/(mol.K)$

t	time, s, h or d
T	temperature, K
z	vertical coordinate, m
Z	gas compressibility factor, -
z_0	height of liquid space, m

References

Amosa, M. K., Mohammed, I. A., Yaro, S. A. (2010). Sulphide scavengers in oil and gas industry – A review. *NAFTA (Zagreb)*, 61: 85-92.

Capek, I. (2004). Preparation of metal nanoparticles in water-in-oil (w/o) microemulsions. *Advances in Colloid and Interface Science*, 110: 49-74. https://doi.org/10.1016/j.cis.2004.02.003.

Crank, J. (1975). *The mathematics of diffusion*. 2nd ed. Oxford, UK: Clarendon Press.

Evers, J. F., Olson, G. A. (1983). *A comparative analysis of reactivities of commercial iron and zinc compounds used in the removal of H_2S from drilling fluids*. Paper SPE 11822. Rocky Mountain Regional Meeting, Salt Lake City, UT. https://doi.org/10.2118/11822-MS.

Husein, M. M., Patruyo, L., Pereira-Almao, P., Nassar, N. N. (2010). Scavenging H_2S(g) from oil phases by means of ultradispersed sorbents. *Journal of Colloid and Interfacial Science*, 342: 253-260. https://doi.org/10.1016/j.jcis.2009.10.059.

International Centre for Diffraction Data. (2023). https://www.icdd.com. (Retreived, November 10, 2023).

Martínez, S. I., Bastidas, C. (2017). *Application of transition metal nanoparticles in the streams production of heavy crude oil treatment: H_2S mitigation*. Paper SPE-185486-MS, SPE Latin America and Caribbean Petroleum Engineering Conference. Buenos Aires, Argentina. https://doi.org/10.2118/185486-MS.

Mi, J., Zhang, B., Shen, Z., Huang, W., Casalins, A. (2017). The experimental study on H_2S generation during thermal recovery process for heavy oil from the Eastern Venezuela Basin. *Journal of Natural Gas Geoscience*, 2: 201-208. https://doi.org/10.1016/j.jnggs.2017.07.003.

Nassar, N. N., Husein, M. M., Pereira-Almao, P. (2010). Ultradispersed particles in heavy oil: Part II, sorption of H_2S(g). *Fuel Processing Technology*, 91: 169-174. https://doi.org/10.1016/j.fuproc.2009.09.008.

Pomeroy, R. D., Lacey, W. N., Scudder, N. F., Stapp, F. P. (1933). Rate of solution of methane in quiescent liquid hydrocarbons. *Industrial and Engineering Chemistry*, 25: 1014-1019. https://doi.org/10.1021/ie50285a021.

Riazi, M. R. (1996). A new method for experimental measurement of diffusion coefficients in reservoir fluids. *Journal of Petroleum Science and Engineering*, 14: 235-250. https://doi.org/10.1016/0920-4105(95)00035-6.

Upreti, S. R., Mehrotra, A. K. (2000). Experimental measurement of gas diffusivity in bitumen: results for carbon dioxide. *Industrial and Engineering Chemistry Research*, 39: 1080-1087. https://doi.org/10.1021/ie990635a.

Upreti, S. R., Mehrotra, A. K. (2002). Diffusivity of CO_2, CH_4, C_2H_6 and N_2 in Atha-

basca bitumen. *Canadian Journal of Chemical Engineering*, 80: 116-125. https://doi.org/10.1002/cjce.5450800112.

Zhang, Y. P., Hyndman, C. L., Maini, B. B. (2000). Measurement of gas diffusivity in heavy oils. *Journal of Petroleum Science and Engineering*, 25: 37-47. https://doi.org/10.1016/S0920-4105(99)00031-5.

Zhu, G., Zhang, S., Huang, H., Liu, Q., Yang, Z., Zhang, J., Wu, T., Huang, Y. (2010). Induced H_2S formation during steams injection recovery processes of heavy oil from the Liaohe Basin, NE China. *Journal or Petroleum Science and Engineering*, 71: 30-36. https://doi.org/10.1016/j.petrol.2010.01.002.